Antifreeze Proteins Bind Independently to Ice

Carl I. DeLuca, Rebecca Comley, and Peter L. Davies
Department of Biochemistry, Queen's University, Kingston, Ontario K7L 3N6, Canada

ABSTRACT   It has been suggested that cooperative interactions between antifreeze proteins (AFPs) on the ice surfaces are required for complete inhibition of ice crystal growth. To test this hypothesis, a 7-kDa type III AFP was linked through its N-terminus to thioredoxin (12 kDa) or maltose-binding protein (42 kDa). The resultant 20-kDa and 50-kDa fusion proteins were larger in diameter than free AFP and thus precluded any extensive AFP-AFP contacts on the ice surface. Both fusion proteins were at least as active as free AFP at virtually all concentrations tested. By these criteria, AFPs function independently of each other and do not require specific intermolecular interactions to bind tightly to ice.

INTRODUCTION

Antifreeze proteins (AFPs) can protect organisms from freezing by binding to ice and inhibiting its growth (Davies and Hew, 1990). This adsorption-inhibition mechanism (Raymond and DeVries, 1977) operates at the ice surface to cause a nonequilibrium lowering of the freezing point below the melting point (thermal hysteresis). Adsorption requires a specific interaction between the ice-binding site of the AFP and a structural feature of the ice lattice. Adsorbed AFPs restrict ice to growing between the bound proteins with a local surface curvature. The increased surface area and curvature make it energetically less favorable for water to join the lattice and results in a local (nonequilibrium) depression of the freezing point (Knight et al., 1991; Wilson, 1993).

It has long been proposed that the basis for adsorption specificity lies in a hydrogen-bonding match between groups on the ice-binding site of the AFP and oxygen atoms on the ice lattice (DeVries and Lin, 1977). For the 37-amino-acid, α-helical type I AFP, seven regularly spaced Thr and Asx have been postulated to be the principal ice-binding residues (DeVries and Lin, 1977; Wen and Laursen, 1992a; Sicheri and Yang, 1995) that result in this AFP's affinity for the $\langle 01\text{−}12 \rangle$ direction of the $\{20\text{−}21\}$ pyramidal plane and their equivalents (Knight et al., 1991), but there is no general agreement about how the AFP docks to this surface. There is concern that the number of hydrogen bonds may be inadequate for the tight binding of mM AFP in the presence of a 10,000-fold molar excess of water (Knight et al., 1993; Wen and Laursen, 1992b). Moreover, x-ray- and NMR-derived structures suggest that the hydrogen bond angles and accessibilities on free AFP might not be optimal for strong binding to ice (Sicheri and Yang, 1995; Gronwald et al., 1996).

Wen and Laursen (1992a) have noted that the relationship between type I AFP concentration ([AFP]) and the inhibition of ice growth is biphasic. At low [AFP] ice grows along both the c and a axes to produce a crystal with a constant c-to-a axis ratio of $\sim$3.3. Above a critical [AFP] (the threshold concentration), the ice crystal ceases to grow and thermal hysteresis is observed. Their explanation for these observations is that AFP binding is reversible at low concentrations because the individual interactions between an AFP and ice are weak. At high concentrations the AFPs begin to bind cooperatively through side-by-side hydrophobic interactions (Wen and Laursen, 1992b). These interpeptide interactions are facilitated by alignment of the helices along the $\langle 01\text{−}12 \rangle$ direction of the $\{20\text{−}21\}$ pyramidal plane, which, according to the model of Wen and Laursen (1992b), brings them into van der Waals contact with each other. In this way, type I AFP binds to ice as a protein patch where the total number of hydrogen bonds linking the AFP to the ice is a multiple of the number of AFPs in the patch.

As a test of this elegant model, Wen and Laursen (1993a) synthesized type I AFP variants that were designed to disrupt side-by-side interactions between the helices. One such variant, in which Ala[17] was replaced by Leu, was completely lacking in thermal hysteresis activity. The bulky aliphatic side chain was calculated to project at right angles to the helix surface containing the putative ice-binding residues and thus sterically interfere with interpeptide interactions. In another test of the model, an all-D-amino acid enantiomer of type I AFP was synthesized and mixed with the natural L-amino acid form. Although the two enantiomers bound to mirror image directions of the same pyramidal plane that would not permit side-by-side packing (Laursen et al., 1994), they did not interfere with each other's activity (Wen and Laursen, 1993b). Nor was there any sign of interference when three different AFPs (types I, II, and III) were mixed (Chao et al., 1995), even though these AFPs are structurally very different (Davies and Sykes, 1997) and bind to different planes of ice (Cheng and DeVries, 1991). The latter results are not inconsistent with the patching hypothesis if each AFP or enantiomer can self-associate to form a homogeneous patch.

A similar bimodal relationship between [AFP] and the inhibition of ice growth has been observed with the 66-amino-acid, globular type III AFP (DeLuca et al., 1996). Furthermore, as was observed for type I AFP, high-resolution x-ray- and NMR-derived structures have suggested that relatively few hydrogen bonds can be made between the AFP and ice and that their enthalpic contribution to binding might be limited by less than optimal bond angles and lengths (Sönnichsen et al., 1996; Jia et al., 1996). These structures have also revealed that the molecule has several flat, orthogonally related surfaces, one of which is the putative ice-binding face. These unusual features of the molecule could theoretically permit side-by-side packing on the ice surface to form an AFP patch with the ice-binding sites aligned for binding to the prism planes. To test the need for cooperativity in type III AFP binding, we have constructed AFP-fusion proteins with an overall diameter far exceeding that of the AFP. In this way, the companion domains would prevent extensive side-by-side interactions of the AFPs. In effect, the fusion proteins did not suffer any loss of thermal hysteresis activity. On the contrary, they were generally more active than the free AFP. These results are consistent with a model in which AFPs bind independently to ice.

MATERIALS AND METHODS

Type III AFP gene modification for cloning into expression plasmids

DNA constructs were made to attach either maltose-binding protein (Kellerman and Ferenci, 1982) or thioredoxin (Holmgren, 1985) to the N-terminus of type III AFP (Fig. 1). To facilitate the cloning, a *Stu*I site was introduced immediately upstream of the *Nde*I site that contains the
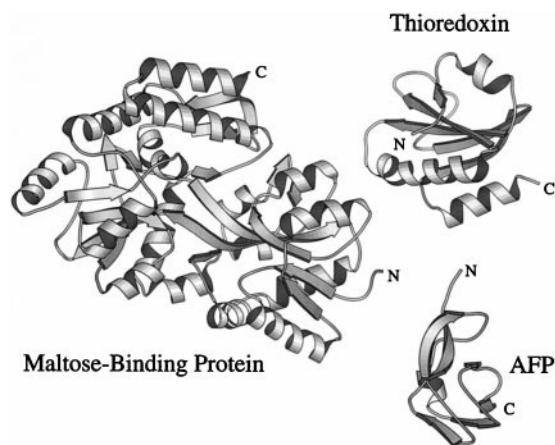

FIGURE 1 Ribbon representation of the structures of Type III AFP, thioredoxin, and maltose-binding protein. The secondary structure was assigned using STRIDE (Frishman and Argos, 1995), and the representations were made with MolScript (Kraulis, 1991). The structures are drawn to the same scale. The amino- and carboxy-termini are labeled N and C, respectively. The design of the fusion protein took into consideration the fact that the ice-binding site on type III AFP is located on the opposite side of the protein from the N-terminus (Chao et al., 1994; Sönnichsen et al., 1996; Jia et al., 1996).

initiating AUG codon of the synthetic AFP gene (Chao et al., 1993). To aid purification of the fusion proteins, the gene for type III AFP was extended to code for six histidines at the C-terminal end of the protein (Janknecht and Nordheim, 1992). The *Stu*I site and the six histidine codons were added simultaneously by oligonucleotide-directed mutagenesis (Kunkel et al., 1987) on single-stranded DNA prepared from the synthetic gene for type III AFP in vector pT7–7f (DeLuca et al., 1993), using oligonucleotides 1 and 2, respectively, where oligonucleotide 1 had the sequence 5′-AA-GAAGGAGATATAGG**CCTCAT**ATGAACCAGG-3′, and oligonucleotide 2 had the sequence 5′-GGTTACGCTGCTCACCACCACCACCAC-CACTAAGAATTCGCGC-3′. The codons in bold indicate the addition of two amino acids (Pro-His) to the linker region as a consequence of introducing the *Stu*I site. Ligated DNA was transformed into competent *Escherichia coli* JM 83, and double mutants were recognized by the presence and absence of *Stu*I and *Afl*II sites, respectively, the latter being lost during the introduction of the histidine codons. The new plasmid was designated pT7–7f*Stu*I:AFP:His-tag.

Construction of a thioredoxin fusion plasmid

The thioredoxin fusion vector was prepared by restriction digestion of pTRXFUS (Invitrogen, San Diego, CA) with *Nde*I and *Pst*I to release a 0.4-kb fragment containing the entire coding region of thioredoxin and the in-frame multiple cloning site. The digested plasmid was electrophoresed on a 1% agarose gel from which the *Nde*I/*Pst*I fragment was eluted by the Prep-A-Gene (BioRad, Hercules, CA) method and ligated to *Nde*I/*Pst*I-digested pT7–7f. Competent *E. coli* JM 83 were transformed with the ligated DNA, and clones were recognized by restriction digestion. The pT7–7f vector containing the thioredoxin gene was designated pT7–7fTRX.

The thioredoxin-type III AFP His-tag fusion gene

The pT7–7f*Stu*I:AFP:His-tag plasmid was digested with *Stu*I and *Cla*I to release a 0.8-kb fragment, which was recovered as described above and digested with *Eco*RI. The *Stu*I/*Eco*RI fragment containing the AFP:His-tag DNA was cloned into *Sma*I/*Eco*RI-digested pT7–7fTR vector. Clones from this ligation were designated pT7–7fTRX:AFP:His-tag. Plasmid DNA was purified from a positive clone and transformed into *E. coli* BL 21 (DE3) cells.

Construction of a maltose-binding protein: type III His-tag fusion gene

The 0.8-kb *Stu*I/*Cla*I fragment from the pT7–7f*Stu*I:AFP:His-tag plasmid was prepared as described above and digested with *Pst*I. The *Stu*I/*Pst*I fragment containing the AFP:His-tag DNA was cloned into *Xmn*I/*Pst*I-digested pMAL-c2 plasmid (New England Biolabs, Beverley, MA) and transformed into competent *E. coli* JM 83. Clones designated as pMal:AFP:His-tag were detected by restriction digestion, and their plasmid DNA was transformed into *E. coli* BL 21 (DE3) cells.

Expression of fusion proteins

LB/amp (100 ml) was inoculated with *E. coli* BL 21 (DE3) containing either the pT7–7fTRX:AFP:His-tag or the pMal:AFP:His-tag fusion plasmid and incubated at 37°C overnight. The inoculum was added to 4 liters of LB/amp for growth at 37°C to an OD_{600} of 0.6, at which point 100 mg/liter of isopropyl-β-D-thiogalactopyranoside was added, and the culture was left for an additional 2 h at 37°C. The cells were pelleted by centrifugation for 60 min at $3500 \times g$ at 4°C, resuspended in 20 mM Tris-HCl (pH 8.0), and broken open by sonication. Particulate matter was removed by centrifugation for 20 min at $12,000 \times g$ at 4°C.

Purification and characterization of fusion proteins

The supernatant from sonication was loaded onto a 5-ml column of Ni-nitrilotriacetic acid (NTA) resin (6 × 1 cm), and the resin was washed with 25 ml of buffer N (10 mM Tris-HCl, 0.5 M NaCl, 5 mM imidazole) at pH 8.0 before elution with 100 mM imidazole-HCl (pH 8.0). Fractions (7 ml) were collected and analyzed by sodium dodecyl sulfate–polyacrylamide gel electrophoresis (SDS-PAGE). The thioredoxin fusion protein was dialyzed against buffer N (3 × 2 liters) and then rechromatographed on the Ni-NTA column. No further purification was required.

After one Ni-NTA column chromatography, the partially purified maltose-binding protein was dialyzed against 10 mM Tris-HCl (pH 8.0) (3 × 2 liters) and loaded at 2.5 ml/min onto a Q-Sepharose Hi-load (Pharmacia, Uppsala, Sweden) column that had been preequilibrated with 10 mM Tris-HCl (pH 8.0). Bound protein was eluted with a linear 0–500 mM NaCl gradient in 10 mM Tris-HCl (pH 8.0) at a flow rate of 2.5 ml/min. Fractions (2.5 ml) containing MBP:AFP:His-tag were pooled and concentrated by ammonium sulfate precipitation (60%). Precipitated protein was pelleted by centrifugation at 12,000 × g for 20 min. The pellet was resuspended in a minimum volume of 50 mM Tris-HCl (pH 8.0) and dialyzed against 50 mM Tris-HCl (pH 8.0) (3 × 1 liter). The dialysate was concentrated with a Centricon 10 while the buffer was exchanged for 100 mM NH_4CO_3. Protein concentrations were routinely estimated by weighing, by the Bradford assay for protein, or by spectrophotometry. The concentrations of stock solutions used for antifreeze activity measurements were determined by amino acid analysis after hydrolysis in 6 N HCl at 160°C for 1.5 h in sealed evacuated tubes. Norleucine was added to the samples as an internal standard. Hydrolyzed material was analyzed in a amino acid analyzer (model 6300; Beckman, San Ramon, CA). The masses of the antifreeze fusion proteins were measured by electrospray mass spectrometry with a Fison VG Quattro mass spectrometer (VG Biotech, Cheshire, England).

Antifreeze activity measurements and photomicroscopy

Thermal hysteresis, defined as the temperature difference (°C) between the melting and nonequilibrium freezing points of a solution, was measured using a nanoliter osmometer (Clifton Technical Physics, Hartford, NY) as described by Chakrabartty and Hew (1991). All measurements were made in 100 mM NH_4HCO_3 (pH 7.9). Ice crystal morphology was observed through a Leitz dialux 22 microscope and recorded with a Panasonic CCTV camera linked to a JVC Super VHS video recorder. Still images were captured with a Silicon Graphics computer and printed on an HP laserjet 4.

RESULTS AND DISCUSSION

Ice crystal growth as a function of type III AFP concentration

Ice crystal growth rates were measured at different type III AFP concentrations by videomicroscopy (Fig. 2). The relationship between c-axis growth rate and [AFP] was qualitatively and quantitatively similar to that obtained by Wen and Laursen (1992a) for type I AFP. There was no crystal growth above a threshold concentration of ~0.06 mM, and growth below the threshold value was proportional to [AFP]. The critical threshold concentration was very close to that reported for type I AFP, even though the two AFPs have very different structures.
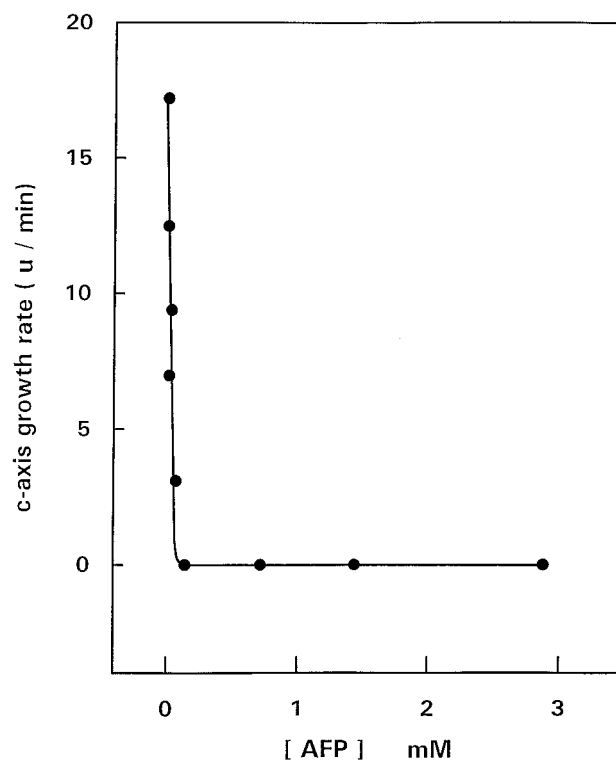
FIGURE 2 Ice crystal growth rates as a function of type III AFP concentration. The rate of crystal growth along the c-axis (μm/min) at an undercooling of 0.2°C was measured over a 10-min interval by videomicroscopy. Each point represents the average of three determinations.

Type III AFP patching possibilities

If the transition between ice growth and no growth is indeed due to patch formation, there should be plausible ways in which the AFPs can self-associate while binding to ice. For type I AFP, alignment of the single α-helix along the $\langle 01\text{--}12 \rangle$ direction of the {20–21} pyramidal plane appears to provide an opportunity for interpeptide interactions along the length of the helix (Wen and Laursen, 1992b). Another attractive feature of this model is that the stagger of the helices can be arrranged such that the helix termini are aligned along the same $\langle -1\text{--}126 \rangle$ direction as the edge of the hexagonal bipyramid. Examination of the 3-D structure of type III AFP (Jia et al., 1996; Sönnichsen et al., 1996) also suggests ways in which this protein could form an ice-binding patch. The relevant structural features are the flatness of the major ice-binding site and the angularity of the AFP. According to the model for type III AFP binding to ice, two ranks of hydrogen bonding atoms on the ice-binding site match oxygen atoms along the $\langle 0001 \rangle$ direction of the {01–01} prism surface. With the AFP bound to ice in this way, several of its adjoining surfaces are remarkably flat and almost perpendicular to the ice surface. In a patching model they might provide enough surface area for adjacent type III AFPs to bind cooperatively through side-by-side interactions. Although the antifreeze was modeled binding to a prism surface and covering the basal plane (Jia

et al., 1996), the flexibility of Asn[14] would allow the anti-freeze to bind just to the prism surface (Sönnichsen et al., 1996). The possibilities for inter-AFP interactions are also increased by the fact that the AFP can rotate through 180° and still bind the $\langle 0001 \rangle$ direction of the $\{01{-}01\}$ prism surface. In short, there are too many permutations to prove or disprove by modeling alone. Therefore, to experimentally test the cooperative binding hypothesis, it was possible to take advantage of the robust, compact nature of type III AFP and the spatial separation of the N- and C-termini from the ice-binding site to add large fusion moieties (Fig. 1) that would sterically block specific AFP-AFP interactions with-out occluding the ice-binding site.

AFP fusion protein isolation

IPTG induction of *E. coli* bearing the AFP fusion protein constructs produced prominent protein bands on SDS-PAGE that were not present in uninduced cells (Fig. 3). The product from the pTRX:AFP:His-tag plasmid had an appar-ent M_r of 20,000 on SDS-PAGE and was by far the most prominent band in the sonicate supernatant. It was substan-tially purified (Fig. 3) by two cycles of binding and step elution from the Ni-NTA agarose affinity column (not shown), with a yield of 5 mg/liter. Its M_r, determined by electrospray mass spectrometry, was 20,782, which agrees well with its predicted value (20,880). Its amino acid com-position (not shown) was consistent with that of the fusion protein.

The new band appearing after IPTG induction of the pMal:AFP:His-tag plasmid had an apparent M_r of 50,000 and was of an intensity equivalent to that of several other proteins in the sonicate supernatant (Fig. 3). This MBP-AFP-His-tag fusion product was largely purified by a single cycle of binding and elution from a Ni-NTA agarose affinity column (not shown). The protein eluted by 0.2 M imidazole was rechromatographed on a cation exchange column to remove minor contaminants. After the second chromatog-raphy, the protein was judged to be pure by SDS-PAGE (Fig. 3), and its yield was 25 mg/liter. It had a M_r of 50,564, as determined by electrospray mass spectrometry, which is close to the predicted value of 50,556 for MBP linked to type III AFP with a His$_6$ extension on the C-terminus. Its amino acid composition (not shown) was also consistent with that of the MBP-AFP-His-tag fusion product. Al-though both AFP fusion proteins have specific affinity chromatography matrices for their purification (namely ThioBond (Invitrogen)) for the thioredoxin fusion and an amylose-agarose composite (NEB) for the MBP fusion, we found that the C-terminal His-tag provided a more conve-nient and reliable method of purification.

AFP-fusion proteins show enhanced thermal hysteresis activity

Concentrated stock solutions of fusion proteins and type III AFP were prepared in 100 mM NH$_4$HCO$_3$ (pH 7.9) and
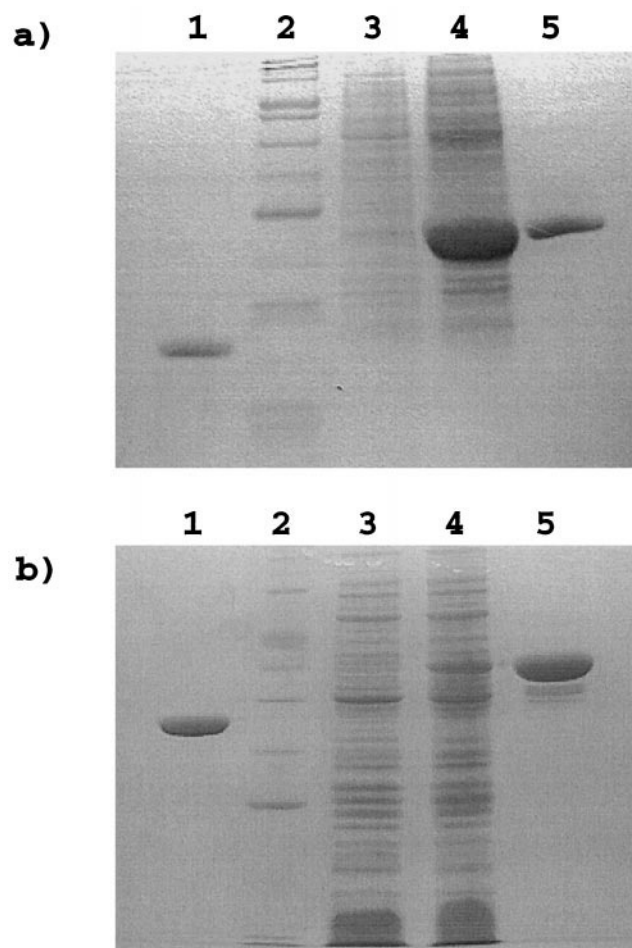

FIGURE 3 SDS-PAGE of fusion protein preparations. (*a*) TRX:AFP:His-tag purification. Lane 1, purified thioredoxin (3 μg); lane 2, M_r standards (Bio-Rad); lanes 3 and 4, preinduced and induced BL21 (DE3) containing pT7–7fTRX:AFP:His-tag, respectively (~250 μl media); lane 5, purified TRX:AFP fusion protein (3 μg). (*b*) MBP:AFP:His-tag purifi-cation. Lane 1, purified maltose-binding protein (3 μg); lane 2, M_r stan-dards (Bio-Rad); lanes 3 and 4, preinduced and induced JM 83 containing pMal:AFP:His-tag, respectively (~250 μl media); lane 5, purified MBP:AFP fusion protein (3 μg).

clarified by centrifugation. The supernatants were used to prepare serial dilutions in 100 mM NH$_4$HCO$_3$ (pH 7.9) for thermal hysteresis measurements over a wide range of con-centrations from μM to mM (Fig. 4, *A* and *B*). At low concentrations, the AFP-fusion proteins were considerably more active than type III AFP on a molar basis. In the range 0–0.5 mM, the two fusion proteins were up to two or three times more active at establishing a given degree of thermal hysteresis than the antifreeze itself (Fig. 4 *B*). The MBP fusion protein had limited solubility, and its solution was close to saturation at 13 mg/ml (0.25 mM). TRX:AFP:His-tag was soluble up to 180 mg/ml (9 mM), and at this concentration had a thermal hysteresis activity of ~2.0°C (Fig. 4 *A*). The most concentrated type III AFP solution obtained (~20 mg/ml or 3 mM) had a thermal hysteresis reading of ~1.4°C. Neither MBP (supplied by B. Shilton, Biotechnology Research Institute, National Research Coun-

a)
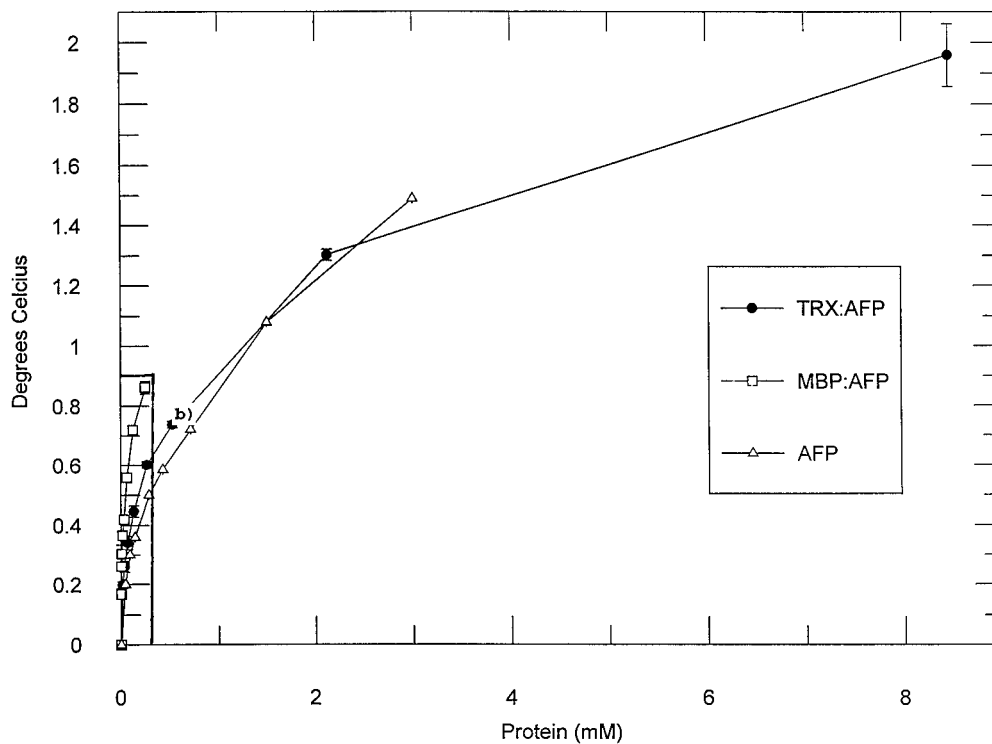
b)

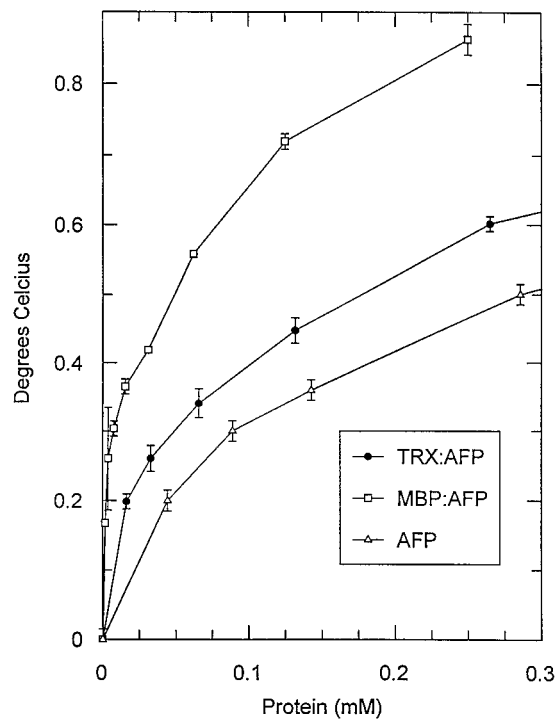FIGURE 4   Activity profile for wild-type and antifreeze fusion proteins. (*a*) The thermal hysteresis activities (°C) of MBP:AFP (□) and TRX:AFP (●) as a function of concentration are compared to that of the wild-type AFP (△). Results are the mean ± SD of triplicate determinations. (*b*) Expansion of *a* in the sub-mM AFP concentration range.

cil of Canada, Montreal, PQ) nor thioredoxin (Invitrogen) showed any antifreeze activity on their own. MBP (20 mg/ml) and TRX (10 mg/ml) were not only devoid of thermal hysteresis activity, but they were also unable to influence the morphology of ice crystals from the uniform disks obtained in the presence of buffer alone (Fig. 5).
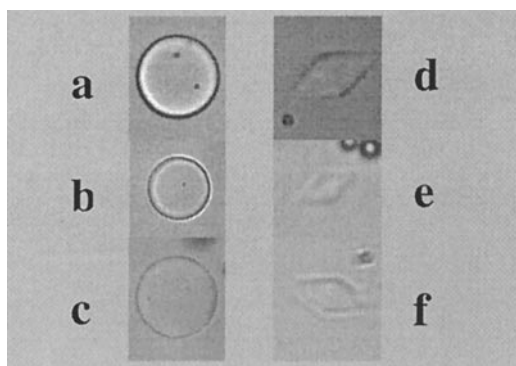
FIGURE 5 Photomicrographs of ice crystals. Ice crystals were formed in the presence and absence of AFP-fusion proteins and their constituents. Ice crystal (*a*) in the absence of protein; (*b*) in the presence of thioredoxin (10 mg/ml) in 100 mM NH_4HCO_3 (pH 7.9); (*c*) in the presence of maltose-binding protein (20 mg/ml) in 100 mM NH_4HCO_3 (pH 7.9). Photographs were taken at 0.02°C of undercooling. The right-hand panel shows ice crystals formed in the presence of 100 mM NH_4HCO_3 (pH 7.9) and mM concentrations of (*d*) wild-type AFP, (*e*) TRX:AFP, and (*f*) MBP:AFP at 0.2°C undercooling.

Rather than eliminating antifreeze activity, the introduction of large companion domains made the AFP more active than the wild-type protein. Despite this change in activity, the ice crystal morphology obtained with the thioredoxin-AFP and MBP-AFP fusion proteins was indistinguishable from that obtained with Type III AFP alone (Fig. 5). It has previously been noted that the three AFP types (I, II, and III) produce different ice crystal morphologies (Chao et al., 1995) that can be attributed to their structural differences (Davies and Hew, 1990) expressed as a preference for binding to different planes of ice (Cheng and DeVries, 1991). The formation of a compound ice-binding site with a contribution from the fusion moiety would be likely to alter the ice crystal morphology from the typical *c*:*a* axis ratio of ~2:1. Because this did not happen with either protein, we conclude that the enhancement of thermal hysteresis does not result from a change in the ice-binding site. Also in this regard, because neither MBP nor thioredoxin showed any antifreeze activity on its own, it can be assumed that the enhanced activity obtained with the fusion proteins was not due to the presence of an additional ice-binding site.

Cooperative AFP-AFP interactions are not required for antifreeze binding to ice

The demonstration that type III AFP fusion proteins are at least as active as the native protein at almost all concentrations tested up to saturation makes a powerful argument for this AFP acting independently at the ice surface. What, then, is the explanation for the biphasic relationship between ice crystal growth and [AFP]? We suggest that this relationship is exactly what would be predicted for an AFP binding independently to ice. At low [AFP] the area between bound AFPs is large enough for water to join easily to the ice lattice and overgrow the adsorbed AFP, because the surface

curvature of the individual ice fronts is slight. Even at these low surface densities, the AFP is bound to a specific plane (and, in some cases, to a specific direction on the plane). These are the principles behind ice etching experiments in which ice hemispheres are grown in dilute AFP solutions and then allowed to sublime to reveal the AFP-binding plane/direction (Knight et al., 1991). As the [AFP] increases, the area of the ice fronts between bound AFP decreases, and the surface curvature needed to overgrow the bound AFP increases. It is this curvature that is the basis for the lowering of the nonequilibrium freezing point according to the Kelvin effect (Wilson, 1993). Our interpretation of the threshold point in Fig. 2 is that it represents the [AFP] at which the surface density of adsorbed AFPs is high enough to ensure that at no point on the ice crystal are AFPs being overgrown (at that particular degree of undercooling). In other words, the area between bound AFPs is small enough to produce adequate curvature on all ice fronts. Above the threshold point, an increase in [AFP] would only serve to decrease the probability of growth. Below the threshold point, the rate at which the ice crystal grows will be related to the surface density of bound AFP (which itself is a function of [AFP] and the rate at which AFP binds to ice).

Concerns that the number and strength of hydrogen bonds between AFP and ice might be insufficient for tight binding have driven the patching hypothesis (Wen and Laursen, 1992b) and one other model (Knight et al., 1993) for increasing the number of hydrogen bonds. Recent results from the 3-D structural analysis of type III AFP (Sönnichsen et al., 1996; Jia et al., 1996) and from type I AFP structure-function analysis (Chao et al., 1997) support the notion that hydrogen bonding alone is perhaps inadequate, but suggest that significant contributions to the energetics of binding may come from van der Waals interactions and entropic solvation effects resulting from the fit of AFP to ice.

Increased activity of AFP-fusion proteins

The Kelvin effect can also be invoked to explain the enhanced activity of the AFP-fusion proteins. We suggest that the AFP fusion proteins are more active, either because each molecule covers more of the ice surface, and/or because it is harder for the ice to grow over them. Again, this is consistent with the model proposed by Wilson (1993) relating freezing point depression to average adsorbant spacing and ice surface distortion. Fig. 6 shows this scenario in diagrammatical form, where the larger fusion protein binding to the ice with the same affinity and surface density would require the ice in between to grow with a more pronounced surface curvature. In the adsorption-inhibition model of macromolecular antifreeze action (Raymond and DeVries, 1977), the lowering of the nonequilibrium freezing point by AFPs is due to the increased energetic costs of adding water to a convex ice surface. Thus an antifreeze that increases ice curvature at the same molar concentration of AFP translates into a more powerful antifreeze.
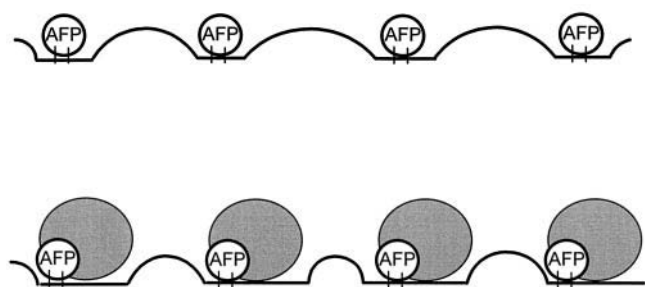
FIGURE 6   Model of antifreeze fusion protein interaction with ice. The presence of a large group attached to the AFP is illustrated as increasing the area covered by the fusion protein and the height of the protein above the ice surface. One consequence is an increased curvature of the ice surfaces between bound AFPs at an equivalent AFP concentration.

Applications for AFP fusion proteins

This work on recombinant AFP fusion proteins contributes to the antifreeze field in two areas. In terms of antifreeze function, it demonstrates that AFPs can function independently at the ice surface, and that cooperativity is not needed for antifreeze activity. It also provides a protein engineering approach to increasing the activity of type III AFP and, by inference, the activity of other AFPs that tolerate N- or C-terminal extensions without occluding the ice-binding site. Thus lower concentrations of AFP fusions can be employed to give the same degree of thermal hysteresis and perhaps inhibition of ice recrystallization. Because the nature of the fusion moiety does not seem to be that important, it could be chosen to facilitate high yields in an expression system or to provide a streamlined purification protocol without the need for subsequent proteolytic removal of the fusion domain. The AFP fusion approach may provide significant advantages in transgenic systems. The addition of large, stable proteins to AFPs may slow their clearance by excretion or degradation. Moreover, fusion of the AFP to selected proteins in the host system may impart localization, tissue and stage specificity, or other beneficial properties deriving from the association with a particular protein. Not only can the fusion increase the activity of Type III AFP; it may also add new functions to the protein.

REFERENCES

Chakrabartty, A., and C. L. Hew. 1991. The effect of enhanced alpha-helicity on the activity of a winter flounder antifreeze polypeptide. *Eur. J. Biochem.* 202:1057–1063.

Chao, H., P. L. Davies, B. D. Sykes, and F. D. Sönnichsen. 1993. Use of proline mutants to help solve the NMR solution structure of type III antifreeze protein. *Protein Sci.* 2:1411–1428.

Chao, H., C. I. DeLuca, and P. L. Davies. 1995. Mixing antifreeze protein types changes ice crystal morohology without affecting antifreeze activity. *FEBS Lett.* 357:183–186.

Chao, H., M. E. Houston, R. S. Hodges, C. M. Kay, B. D. Sykes, M. C. Loewen, P. L. Davies, and F. D. Sönnichsen. 1997. A diminished role for hydrogen bonds in antifreeze protein binding to ice. *Biochemistry.* 36:14652–14660.

Chao, H., F. D. Sönnichsen, C. I. DeLuca, B. D. Sykes, and P. L. Davies. 1994. Structure-function relationship in the globular type III antifreeze protein: identification of a cluster of surface residues required for binding to ice. *Protein Sci.* 3:1760–1769.

Cheng, C. C., and A. L. DeVries. 1991. The role of antifreeze glycopeptides and peptides in the freezing avoidance of cold-water fish. *In* Life under Extreme Conditions. G. di Prisco, editor. Springer-Verlag, Berlin. 1–14.

Davies, P. L., and C. L. Hew. 1990. Biochemistry of fish antifreeze proteins. *FASEB J.* 4:2460–2468.

Davies, P. L., and B. D. Sykes. 1997. Antifreeze proteins. *Curr. Opin. Struct. Biol.* 7:828–834.

DeLuca, C. I., H. Chao, F. D. Sönnichsen, B. D. Sykes, and P. L. Davies. 1996. Effect of type III antifreeze protein dilution and mutation on the growth inhibition of ice. *Biophys. J.* 71:2346–2355.

DeLuca, C. I., P. L. Davies, J. A. Samis, and J. S. Elce. 1993. Molecular cloning and bacterial expression of cDNA for rat calpain II 80 kDa subunit. *Biochim. Biophys. Acta.* 121:81–93.

DeVries, A. L., and Y. Lin. 1977. Structure of a peptide antifreeze and mechanisms of absorption to ice. *Biochim. Biophys. Acta.* 495:380–392.

Frishman, D., and P. Argos. 1995. Knowledge-based secondary structure assignment. *Proteins Struct. Funct. Genet.* 23:566–579.

Gronwald, W., H. Chao, D. V. Reddy, P. L. Davies, B. D. Sykes, and F. D. Sönnichsen. 1996. NMR characterization of side-chain flexibility and backbone structure in the type I antifreeze protein near freezing temperatures. *Biochemistry.* 35:16698–16704.

Holmgren, A. 1985. Thioredoxin. *Annu. Rev. Biochem.* 54:237–271.

Janknecht, R., and A. Nordheim. 1992. Affinity purification of histidine-tagged proteins transiently produced in HeLa cells. *Gene.* 121:321–324.

Jia, Z., C. I. DeLuca, H. Chao, and P. L. Davies. 1996. Structural basis for a globular antifreeze protein binding to ice. *Nature.* 284:285–288.

Kellerman, O. K., and T. Ferenci. 1982. Maltose-binding protein from *E. coli. Methods Enzymol.* 90:459–463.

Knight, C. A., C. C. Cheng, and A. L. DeVries. 1991. Adsorption of α-helical antifreeze peptides on specific ice crystal surface planes. *Biophys. J.* 59:409–418.

Knight, C. A., E. Driggers, and A. L. DeVries. 1993. Adsorption to ice of fish antifreeze glycopeptides 7 and 8. *Biophys. J.* 64:252–259.

Kraulis, P. J. 1991. MOLSCRIPT: a program to produce both detailed and schematic plot of protein structures. *J. Appl. Crystallogr.* 24:946–950.

Kunkel, T. A., J. D. Roberts, and R. A. Zarkour. 1987. Rapid and efficient site-specific mutagenesis without phenotypic selection. *Methods Enzymol.* 154:367–382.

Laursen, R. A., D. Wen, and C. A. Knight. 1994. Enantioselective adsorption of the D- and L-forms of an α-helical antifreeze polypeptide to the {20–21} planes of ice. *J. Am. Chem. Soc.* 116:12057–12508.

Raymond, J. A., and A. L. DeVries. 1977. Adsorption inhibition as a mechanism of freezing resistance in polar fishes. *Proc. Natl. Acad. Sci. USA.* 74:2589–2593.

Sicheri, F., and D. S. C. Yang. 1995. Ice-binding structure and mechanism of an antifreeze protein from winter flounder. *Nature.* 375:427–431.

Sönnichsen, F. D., C. I. DeLuca, P. L. Davies, and B. D. Sykes. 1996. Refined solution structure of type III antifreeze protein: a possible involvement of hydrophobic groups in the energetics of the protein-ice interaction. *Structure.* 4:1325–1337.

Wen, D., and R. A. Laursen. 1992a. Structure-function relationships in an antifreeze polypeptide. *J. Biol. Chem.* 267:14102–14108.

Wen, D., and R. A. Laursen. 1992b. A model for binding of an antifreeze polypeptide to ice. *Biophys. J.* 63:1659–1662.

Wen, D., and R. A. Laursen. 1993a. Structure-function relationships in an antifreeze polypeptide: the effect of added bulky groups on activity. *J. Biol. Chem.* 268:16401–16405.

Wen, D., and R. A. Laursen. 1993b. A D-antifreeze polypeptide displays the same activity as its natural L-enantiomer. *FEBS lett.* 317:31–34.

Wilson, P. W. 1993. Explaining thermal hysteresis by the Kelvin effect. *Cryo-Letters.* 14:31–36.